

Scientific paper

# Liquid/Single Crystal Structure Analysis: Synthesis and Characterization of a Trimethylsilyl Derived Rod Shaped Mesogen

Hosapalya Thimmaiah Srinivasa,<sup>1,2</sup> Bandrehalli Siddagangappa Palakshamurthy,<sup>3</sup>  
Devadasan Velmurugan,<sup>4</sup> Hirihalli Chickegowda Devarajegowda<sup>3</sup>  
and Suresh HariPrasad\*<sup>1</sup>

<sup>1</sup> Department of Chemistry, Bangalore University, Bengaluru-560001, Karnataka, India

<sup>2</sup> Raman Research Institute, Sadashivanagar, Bengaluru-560080, Karnataka, India

<sup>3</sup> Department of Physics, Yuvaraja's College (Constituent College), University of Mysore, Mysuru-570005, Karnataka, India

<sup>4</sup> CAS in Crystallography and Bio-physics, University of Madras, Guindy Campus, Chennai-600025, Tamilnadu, India

\* Corresponding author: E-mail: hariprasad@bub.ernet.in

Phone: +918022961351; Fax: +918022961331

Received: 17-02-2015

## Abstract

4-[4'-Cyanophenoxy-carbonyl-phenyl-4-(trimethylsilyl)ethynyl]benzoate a rod shaped liquid crystal (SmA) is synthesized and characterized. The single-crystals were grown in triclinic crystal system in the space group of  $P\bar{1}$  with unit cell parameters  $a = 5.9577(2)$  Å,  $b = 8.0398(3)$  Å,  $c = 25.8842(9)$  Å,  $\alpha = 86.096(2)^\circ$ ,  $\beta = 89.912(2)^\circ$ ,  $\gamma = 2.919(2)^\circ$ ,  $Z = 2$ , and  $V = 1182.16(7)$ . The crystal structure is stabilized by C–H $\cdots$ O intra-molecular interactions. Further, the structure also involves C–H $\cdots\pi$  interactions and weak  $\pi$ – $\pi$  stacking interactions [centroid–centroid separation = 3.806 (3) Å].

**Keywords:** Trimethylsilyl benzoates, Single crystal, Liquid crystal, Mesophase, Smectic phase.

## 1. Introduction

Liquid crystal displays (LCDs) have shown a significant capability to spatially manipulate the phase information of an incidental beam of light. This technology is widely applied in a large number of optical applications and hence they have been employed as spatial light modulators (SLMs) in image processing, holography, data storage, programmable adaptive optics, medical optics, and diffractive optics.<sup>1</sup> Recently, a new type of reflective LCDs has been developed by employing liquid crystals of silicon (LCoS). These displays have awakened a great amount of interest among researchers due to their specific technical characteristics, which are superior in many aspects to the ones provided by transmissive LCDs.<sup>2</sup> For example, as LCoS displays work in reflection, the light impinging such devices perform a double pass through the liquid crystal cell, which leads to a larger phase modulation

than that of the one related to transmissive LCDs with the same thickness. This greater phase modulation capability allows LCoS displays to become very suitable devices for digital holography applications like laser beam shaping and optical micro-particle manipulation.<sup>3</sup>

Designing of thermotropic liquid crystals with terminal trimethylsilylacetylene and siloxane units in the core is gaining prominence due to the application of silicon liquid crystals.<sup>4</sup> This could be attributed to the presence of terminal acetylene unit, which strongly influences mesophase characteristics by bringing in considerable changes in polarity, polarizability, geometry and birefringence properties of the molecule.<sup>5,6</sup> Siloxane units are used for the purpose of building mesogens and have attracted prime attention owing to its applications in the form of alignment studies and optical studies.<sup>7,8</sup> From the point of molecular structure, it is observed that the insertion of trimethylsilyl group into the mesogenic core can substantially influence the optical anisotropy

and considerably reduce the melting transition temperature due to the tetrahedron geometry of bulky trimethylsilyl group.<sup>9,10</sup> In addition, studies have revealed that trimethylsilyl based mesogens possess a strong hydrophobicity and promote liquidity in general leading to reduction in viscosity.<sup>11</sup> Thus, establishing a relationship between mesogenic structure and the magnitude of the polarizability, anisotropy in trimethylsilyl mesogens is very crucial both for regulating and optimization of optical properties.<sup>12–15</sup>

Our laboratory is involved in the synthesis, study of reactions and application of organosilyl based compounds.<sup>16</sup> In continuation of our studies, we were further interested in the synthesis and examination of compounds which possess mesogenic properties as well as single crystal properties. There exist no reports of compounds bearing trimethylsilyl and polar cyano group derived molecules as liquid crystals. Keeping this in mind we hereby report the synthesis, mesomorphic characterization and X-ray single crystal studies of 4-[4'-cyanophenoxy-carbonyl-phenyl-4-(trimethylsilyl) ethynyl] benzoate.

## 2. Experimental

### 2.1. Materials

All chemicals were purchased from Sigma-Aldrich and Merck and used as received. Solvents were distilled and dried prior to the reactions. Single crystals suitable for X-ray diffraction studies were obtained by slow evaporation of hexane at room temperature.

### 2.2. Instruments and Experiments

All the reactions were monitored by thin layer chromatography using Merck silica gel pre-coated on aluminium sheets with 1:4 ratio ethyl acetate and petroleum benzene (60–80 °C fraction) as mobile phase. The products were purified by column chromatography on Acme make silica gel 60–120 mesh size. The chemical structures were confirmed by <sup>1</sup>H-NMR spectroscopy (Bruker Biospin 500MHz spectrometer), and FTIR spectroscopy (Shimadzu FTIR-8400 spectrometer). The purities of the compounds were established by elemental analysis performed on Carlo-Erba 1106 analyzer. The thermal behavior was investigated by Differential Scanning Calorimetry (DSC) using a Perkin-Elmer, Pyris 1 calibrated using indium and zinc standards. The mesophase characterization of liquid crystal textures were performed by BX50 Olympus Polarized Optical Microscope (POM) equipped with a temperature controlled Mettler FP82HT hot stage and Mettler FP90 central processor. Thermal stability was established by Perkin Elmer TGA4000 analyzer. The heating and cooling profiles were done at the rate of 10 °C min<sup>-1</sup>. X-ray diffraction studies were performed on non-oriented samples filled using Lindeman capillary, diameter of 1.0 mm using Cu-K $\alpha$  (0.154 nm) radiation from a rotating anode X-ray generator

(Rigaku Ultrax-18) operating at 50 kV and 80 mA. Two-dimensional detector Image Plate from Mar Research was used for the collection of scattered radiation.

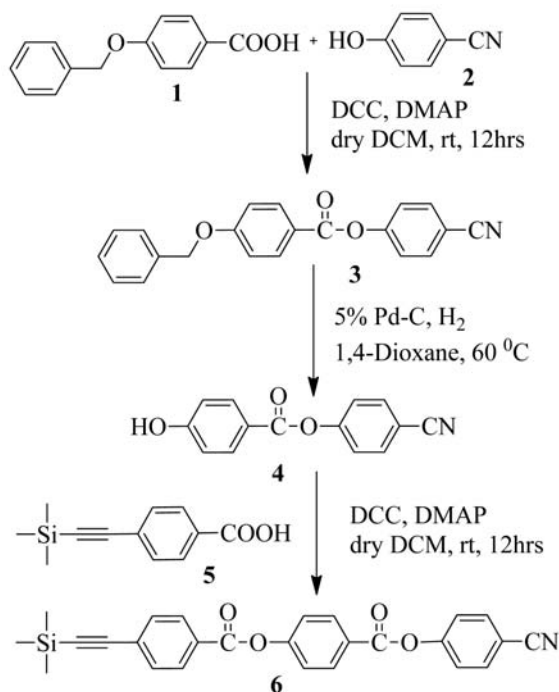
## 3. Results and Discussion

### 3.1. Synthesis

4-Benzyloxybenzoic acid (**1**) was condensed with 4-cyanophenol (**2**) using the simple esterification method to get protected intermediate (**3**). Hydrogenolysis on 5% Pd-C catalyst offered 4-cyanophenyl-4'-hydroxybenzoate (**4**) according to reported literature procedure.<sup>17</sup> The intermediate 4-[2-(trimethylsilyl)ethynyl]benzoic acid (**5**) was prepared by Sonogashira coupling reaction with 4-iodobenzoic acid. The title compound (**6**) was prepared by the condensation of **4** and **5** using the cross coupling agent *N,N*-dicyclohexylcarbodiimide (DCC) in presence of 4-(*N,N*-dimethylamino) pyridine (DMAP) catalyst and dichloromethane solvent as shown in Scheme 1.

#### 3.1.1. 4-[4'-Cyanophenoxy-carbonyl-phenyl-4-(trimethylsilyl)ethynyl]benzoate (**6**).<sup>18</sup>

4-Cyanophenyl-4'-hydroxybenzoate (**4**) (0.290 g, 1.00 mmol) and 4-[2-(trimethylsilyl) ethynyl]benzoic acid (**5**) (0.0570 g, 1.1 mmol) were dissolved in 10 ml of dry dichloromethane. Then, DCC (0.226 g, 1.10 mmol) and DMAP (0.013 g, 0.11 mmol) were added and the mixture was stirred for 12 hrs at room temperature. The reaction progress was monitored by TLC. After the completion of



Scheme 1. Synthetic scheme for the compound **6**.

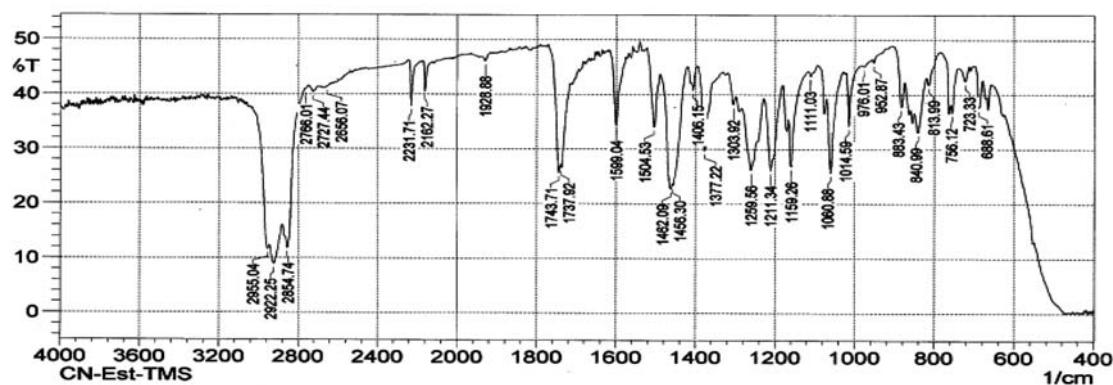


Figure 1. FT-IR spectrum of 4-[4'-cyanophenoxy-carbonyl-phenyl-4-(trimethylsilyl)ethynyl]-benzoate (**6**).

reaction, the reaction mixture was poured into ice-water. The dicyclohexyl urea precipitate was removed by filtration. The filtrate was separated and concentrated *in-vacuo*. The residual solid was re-dissolved in dichloromethane. The organic phase was washed with diluted acetic acid and water and the solvent removed under reduced pressure. The compound was purified on silica gel by column chromatography using dichloromethane/hexane as an eluent. Recrystallization from hexane gave the target compound **6**. Yield: 0.112 g, 34%.

4-[4'-Cyanophenoxy-carbonyl-phenyl-4-(trimethylsilyl)ethynyl]benzoate (**6**) IR: 2922, 2854, 2231, 2162, 1743, 1599, 1462, 1259, 1060, 756  $\text{cm}^{-1}$ ;  $^1\text{H-NMR}$ : 8.12 (d, 2H,  $J = 8.6$  Hz, Ar-H), 7.95 (d, 2H,  $J = 8.5$  Hz, Ar-H), 7.63–7.44 (dd, 4H,  $J = 8.4$  & 8.6 Hz, Ar-H), 7.22 (m, 4H, Ar-H), 0.30 (s, 9H,  $-\text{Si}(\text{CH}_3)_3$ ); Elemental analysis  $\text{C}_{26}\text{H}_{21}\text{NO}_4\text{Si}$  requires C, 71.05; H, 4.82; N, 3.19; found C, 71.13; H, 4.94; N, 3.10.

The FT-IR spectrum of **6** is shown in Figure 1. The peaks observed at 2231  $\text{cm}^{-1}$ , 2152  $\text{cm}^{-1}$  and 1743  $\text{cm}^{-1}$  are assigned to the stretching of cyano-, acetylene- and ester functional groups respectively.

Table 1. Phase transition temperatures ( $T/^\circ\text{C}$ ) and associated enthalpy values in square brackets ( $\Delta H/\text{kJ mol}^{-1}$ ) of 4-[4'-cyanophenoxy-carbonyl-phenyl-4-(trimethylsilyl)ethynyl]benzoate (**6**).

Compound	Heating scan	Cooling scan
<b>6</b>	Cr 156.3 [66.4] SmA 162.1 [4.1] Iso	Iso 161.1 [4.0] SmA 107.4 [67.9] Cr

In order to confirm the chemical composition of the synthesized compound carbon (C), hydrogen (H) and nitrogen (N) analysis was carried out. The experimental and calculated percentages of C, H, and N are given in analysis data. The differences between experimental and calculated percentages of C, H, and N were very close to each other and within the accepted errors. This confirmed the formation of the product **6**.

### 3. 1. 2. Mesomorphic Studies

Thermal behavior of compound **6** was evaluated in conjunction with polarizing optical microscope (POM),

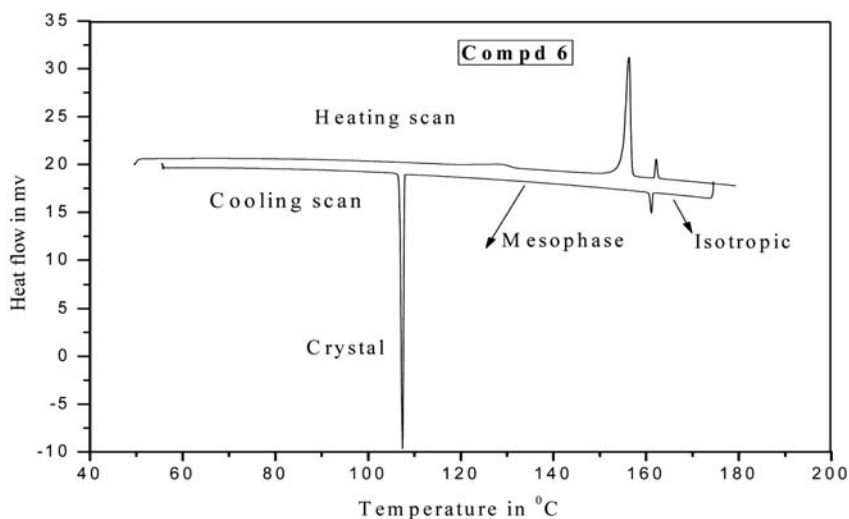


Figure 2. DSC scan of 4-[4'-cyanophenoxy-carbonyl-phenyl-4-(trimethylsilyl)ethynyl]-benzoate.

differential scanning calorimeter (DSC) and the transition temperatures gathered from calorimeter measurements of first heating and cooling scanned at rate of 5 °C/min. The results of our observations are tabulated in Table 1.

The title compound exhibit enantiotropic Smectic A phase is confirmed by DSC and POM studies. The DSC scan of compound **6** is shown in Figure 2.

The compound **6** melts at temperature 156.3 °C with enthalpy  $\Delta H$  (66.4) from crystal to Smectic phase and it went isotropic state at 162.1 °C ( $\Delta H$  4.1), and the same sample cooled from isotropic state the Smectic phase reappears at 161.1 °C ( $\Delta H$  4.0) then it crystallizes at 107.4°C ( $\Delta H$  67.9) from liquid crystal state.

The POM studies were carried out by sandwiching the sample between untreated glass plate and cover slip. The sample was heated to its isotropic state, and then the sample upon cooling showed characteristic fan shaped texture for typical Smectic phase. The POM pictures are shown in Figure 3(a) taken at early growing state of Smectic phase and Figure 3(b) is taken at complete grown liquid crystal state.

### 3. 1. 3. X-ray Studies at Liquid Crystalline State

We have studied the X-ray diffraction at 140 °C. The X-ray intensity versus  $2\theta$  pattern is shown in Figure

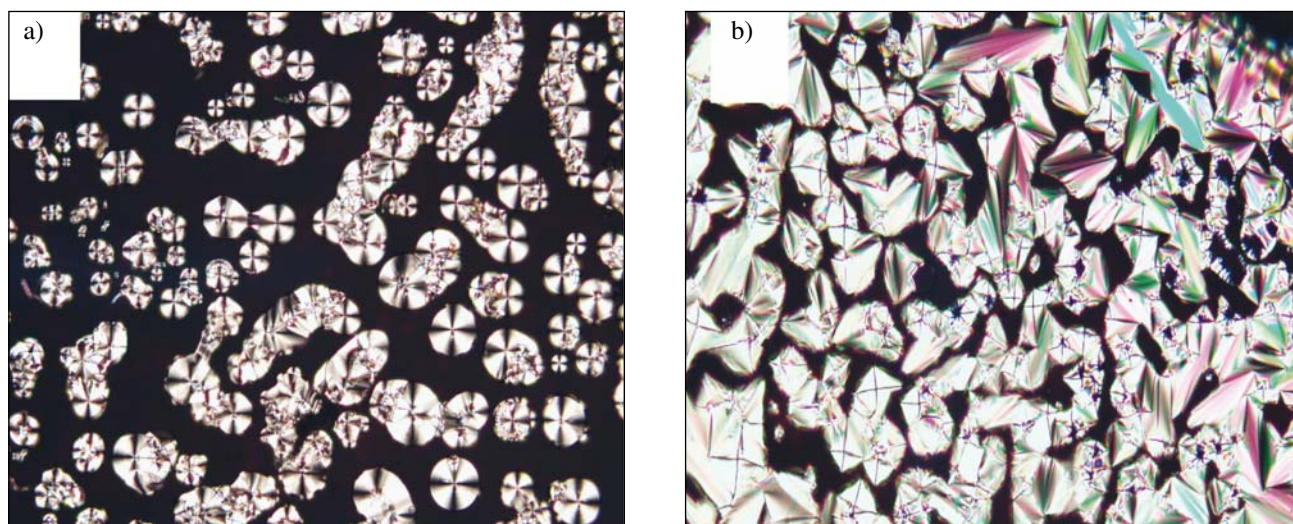


Figure 3. Polarized Optical Micrographs of 4-[4'-Cyanophenoxy-carbonyl-phenyl-4-(trimethylsilyl)ethynyl]benzoate **6**.

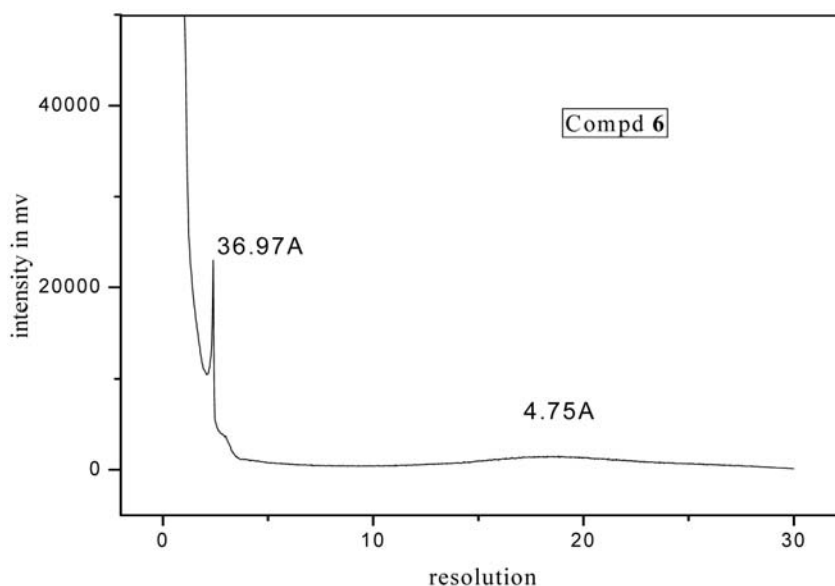


Figure 4. X-ray scan at liquid crystal state for 4-[4'-cyanophenoxy-carbonyl-phenyl-4-(trimethylsilyl)ethynyl]benzoate.

re 4. The X-ray diffraction pattern has a sharp peak in the small-angle region with d-spacing of about 36.97 Å, and an additional broad peak in the wide-angle region with d-spacing of about 4.75 Å, reflecting the liquid-like arrangement of the molecules within each layer. Length of the molecule was also estimated from energy-minimized structure using ChemDraw software. The average length of the molecule was  $L = 36.89$  Å, which suggests that  $L$  was parallel to the Smectic layer and that normal and flexible chains were randomly oriented in the plane of the Smectic in its stretched conformation.

### 3. 1. 4. Single Crystal X-ray Diffraction Method

Single crystals of size  $0.1 \times 0.2 \times 0.3$  mm were selected under a polarizing microscope and affixed to Hampton research cryoloop using paratone oil for data collection. The X-ray diffraction data sets were collected

**Table 3.** Bond lengths (Å), of the title compound.

Atom–Atom	Bond length	Atom–Atom	Bond length
C25–Si1	1.834(3)	C12–C13	1.380(3)
C26–Si1	1.808(4)	C12–O3	1.397(2)
C1–N1	1.133(3)	C12–O3	1.397(2)
C1–C2	1.443(3)	C13–C14	1.370(3)
C2–C3	1.379(3)	C15–O4	1.188(3)
C2–C7	1.382(3)	C15–O3	1.362(2)
C3–C4	1.378(3)	C15–C16	1.480(3)
C4–C5	1.373(3)	C16–C17	1.376(3)
C5–C6	1.375(3)	C16–C21	1.389(3)
C5–O1	1.399(2)	C17–C18	1.376(3)
C6–C7	1.373(3)	C18–C19	1.386(3)
C8–O1	1.358(2)	C19–C20	1.389(3)
C8–C9	1.485(3)	C19–C22	1.444(3)
C9–C14	1.389(3)	C20–C21	1.374(3)
C8–O2	1.189(2)	C22–C23	1.190(3)
C9–C10	1.389(3)	C23–Si1	1.831(2)
C10–C11	1.378(3)	C24–Si1	1.857(3)
C11–C12	1.374(3)		

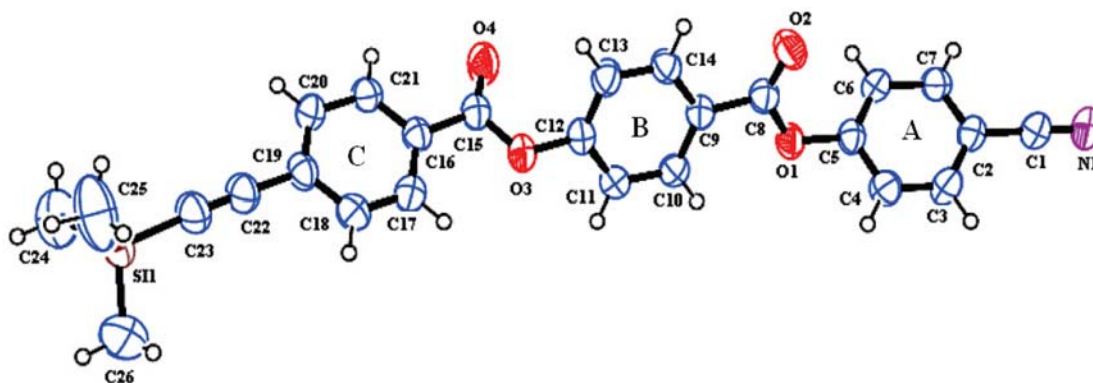


**Figure 5.** The ORTEP diagram of the molecule with 50% probability displacement thermal ellipsoids.

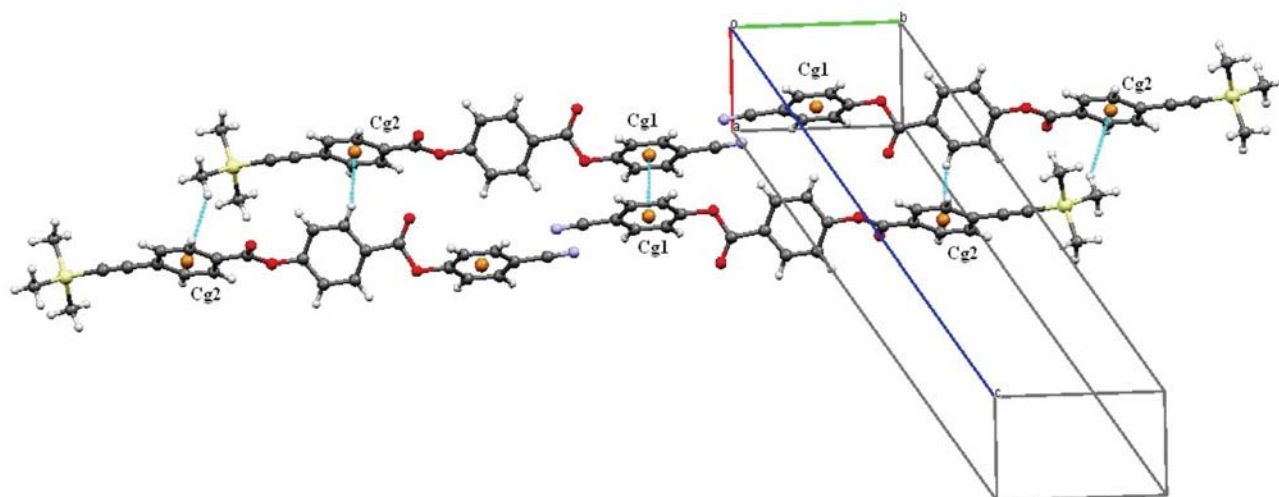


**Figure 6.** The packing diagrams depicting the C...H intermolecular interactions.

on a Bruker SMART CCD diffractometer using Mo K $\alpha$  radiation. The crystal-to-detector distance was fixed at 40 mm. The scan width per frame was  $\Delta\omega = 0.5^\circ$ . The cell refinement and data reduction were carried out using the SAINT<sup>19</sup>. The crystal structures were solved by direct methods using SHELXS97<sup>20</sup> and refined in the spherical-atom approximation (based on *F*<sup>2</sup>) by using SHELXL2014<sup>21</sup>. The ORTEP diagrams (Figure 5) and packing diagram (Figure 6) is generated using ortep3v2<sup>22</sup> and Mercury.<sup>23</sup> The experimental and all crystallographic data, including structure refinement details are reported in Table 2 (Supplementary Information). A few bond lengths, bond angles, torsion angles, and Hydrogen-bond are reported in Table 3, 4, 5 and 6 respectively.

The dihedral angle between the aromatic rings A B, A C, and B C are 50.47(1)°, 10.51(2)° and 50.02(1)° respectively. In the extended structure the molecular packing is stabilized by C10–H10...O1, C17–H17...O3 and C14–H14...Cg2, C24–H24...Cg2 interactions. Further a weak  $\pi$ – $\pi$  stacking interaction is also observed [centroid–centroid separation = 3.806 (3) Å].

According to theory the C–C single bond length is 1.54 Å. In the case of Si–C and Si = C bonds distances are 1.89 Å and 1.72 Å respectively. The experimentally determined data indicates that the Si–C bond length is between 1.808 to 1.857 Å, which is good agreement with the theoretical values.

**Table 4.** Bond angles (°) of the title compound.

Atom–Atom–Atom	Angle	Atom–Atom–Atom	Angle
N1–C1–C2	177.4(3)	C3–C2–C7	120.35(19)
C7–C2–C1	120.7(2)	C4–C3–C2	120.13(19)
C5–C4–C3	118.5(2)	C13–C12–O3	121.50(18)
C14–C13–C12	118.82(19)	C13–C14–C9	121.0(2)
O4–C15–O3	123.34(19)	O4–C15–C16	125.3(2)
O3–C15–C16	111.36(19)	C17–C16–C21	119.44(19)
C17–C16–C15	123.10(19)	C21–C16–C15	117.46(19)
C16–C17–C18	120.3(2)	C17–C18–C19	120.7(2)
C4–C5–C6	122.12(18)	C1–C5–O1	116.21(18)
C6–C5–O1	121.61(18)	C7–C6–C5	118.91(19)
C6–C7–C2	119.8(2)	O2–C8–O1	123.52(18)
O2–C8–C9	125.08(19)	O1–C8–C9	111.39(17)
C14–C9–C10	119.17(18)	C14–C9–C8	117.02(18)
C10–C9–C8	123.79(18)	C11–C10–C9	120.08(18)
C12–C11–C10	119.52(19)	C11–C12–C13	121.37(19)
C11–C12–O3	116.96(18)	C13–C12–O3	121.50(18)
C11–C12–O3	116.96(18)	C18–C19–C20	118.76(19)
C18–C19–C22	119.3(2)	C20–C19–C22	121.9(2)
C21–C20–C19	120.53(19)	C20–C21–C16	120.2(2)
C23–C22–C19	178.0(3)	C22–C23–Si1	177.2(2)
C8–O1–C5	117.50(15)	C15–O3–C12	119.49(17)
C26–Si1–C23	107.57(15)	C26–Si1–C25	113.8(3)
C23–Si1–C25	109.52(14)	C26–Si1–C24	109.5(3)
C23–Si1–C24	108.74(15)	C25–Si1–C24	107.60(17)

**Table 5.** Selected torsion angles (°) of the title compound.

Atom–Atom–Atom–Atom	Angle
N1–C1–C2–C3	–61(6)
N1–C1–C2–C7	117(5)
C7–C2–C3–C4	–2.8(3)
C1–C2–C3–C4	175.19(19)
C2–C3–C4–C5	0.4(3)
C3–C4–C5–C6	2.5(3)
C3–C4–C5–O1	179.83(17)
C4–C5–C6–C7	–3.0(3)
O1–C5–C6–C7	179.85(17)
C5–C6–C7–C2	0.5(3)
C3–C2–C7–C6	2.4(3)
C1–C2–C7–C6	–175.63(19)
O2–C8–C9–C14	7.1(3)
O1–C8–C9–C14	–173.63(17)
O2–C8–C9–C10	–171.5(2)
O1–C8–C9–C10	7.7(3)
C14–C9–C10–C11	0.4(3)
C8–C9–C10–C11	179.06(18)
O3–C15–C16–C21	175.68(17)
C21–C16–C17–C18	–1.2(3)
C15–C16–C17–C18	178.42(19)
C16–C17–C18–C19	0.4(3)
C17–C18–C19–C20	0.2(3)
C17–C18–C19–C22	178.4(2)
C18–C19–C20–C21	–0.2(3)
C22–C19–C20–C21	–178.28(19)
C19–C20–C21–C16	–0.6(3)
C17–C16–C21–C20	1.3(3)
C15–C16–C21–C20	–178.36(18)
C18–C19–C22–C23	18(8)
C20–C19–C22–C23	–164(8)
C19–C22–C23–CSi1	–65(11)
O2–C8–O1–C5	8.3(3)
C9–C8–O1–C5	–170.98(16)
C4–C5–O1–C8	120(2)

**Table 6.** Hydrogen-bond geometry of the molecule in (Å, °), Cg2 – is the centroid for the ring C16/C17/C18/ C19 /C20 /C21

D–H...A	D–H	H...A	D...A	D–H...A
C10–H10...O1	0.93	2.46	2.760(2)	98.9
C17–H17...O3	0.93	2.42	2.732(3)	99.7
C14–H14...Cg2	0.93	2.80	3.414(2)	124
C24–H24C...Cg2	0.93	2.99	3.797(4)	143

## 4. Conclusions

The synthesis and analysis of 4-[4'-cyanophenoxy-carbonyl-phenyl-4-(trimethylsilyl)ethynyl]benzoate is reported. The three phenyl ring core exhibited enantiotropic Smectic A phase. The single crystal X-ray diffraction studies shows that the title compound crystallizes in triclinic system. The crystal structure is stabilized by C–H...O intra-molecular and C–H... $\pi$  interactions and also by  $\pi$ ... $\pi$  interactions [centroid–centroid separation = 3.806 (3) Å].

## 5. Supplementary Data

CCDC 1057495 contains the supplementary crystallographic data for compound **6**. The data can be obtained free of charge via <http://www.ccdc.cam.ac.uk/conts/retrieving.html>, or from the Cambridge Crystallographic Data Centre, 12 Union Road, Cambridge CB2 1EZ, UK; fax: (+44) 1223-336-033; or e-mail: [deposit@ccdc.cam.ac.uk](mailto:deposit@ccdc.cam.ac.uk).

## 6. References

1. A. Lizana, L. Lobato, A. Marquez, C. Iemmi, I. Moreno, J. Campos, M. J. Yzuel, Chapter 11, in *Advanced Holography - Metrology and Imaging*, In Tech; **2011**. I. Naydenova (Ed.), DOI: 10.5772/18668. <http://dx.doi.org/10.5772/18668>
2. Y. Lee, J. Gourlay, W. J. Hossack, I. Underwood, A. J. Walton, *Optics Commun.* **2004**, *236*, 313–322. <http://dx.doi.org/10.1016/j.optcom.2004.03.043>
3. W.P. Bleha, L. A. Lei, *Proc. of SPIE*, **2013**, *8736*, 87360A-2. <http://dx.doi.org/10.1117/12.2015973>
4. C. T. Liao, Z. L. Wu, N. C. Wu, J. Y. Liu, M. H. Jiang, S. F. Zou, J. Y. Lee, *Mol. Cryst. Liq. Cryst.* **2010**, *533*, 3–15. <http://dx.doi.org/10.1080/15421406.2010.504507>
5. C. H. Ting, J. T. Chen, C. S. Hsu, *Macromolecules*, **2002**, *35*, 1180–1189. <http://dx.doi.org/10.1021/ma0107962>
6. Y. Arakawa, S. Nakajima, R. Ishige, M. Uchimura, S. Kang, G. Konishi, J. Watanabe, *J. Mater. Chem.* **2012**, *22*, 8394–8398. <http://dx.doi.org/10.1039/c2jm16002a>
7. Q. S. Hu, V. Pugh, M. Sabat, L. Pu, *J. Org. Chem.* **1999**, *64*, 7528–7536. <http://dx.doi.org/10.1021/jo990856q>
8. T. M. Long, T. M. Swager, *J. Mat. Chem.* **2002**, *12*, 3407–3412. <http://dx.doi.org/10.1039/b203160d>
9. G. Hennrich, P. D. Ortiz, E. Cavero, R. E. Hanes, J. L. Serrano, *Eur. J. Org. Chem.* **2008**, *27*, 4575–4579. <http://dx.doi.org/10.1002/ejoc.200800568>
10. T. Hanasaki, Y. Kamei, A. Mandai, K. Uno, K. Kaneko, *Liq. Cryst.* **2011**, *38*, 841–848. <http://dx.doi.org/10.1080/02678292.2011.583994>
11. E. B. Florjanczyk, J. T. Soltysiak, *J. Organomet. Chem.* **2010**, *695*, 1911–1917. <http://dx.doi.org/10.1016/j.jorganchem.2010.04.025>
12. J. Lu, M. Tian, Q. Chen, J. Wen, *Liq. Cryst.* **1995**, *18*, 101–103. <http://dx.doi.org/10.1080/02678299508036597>
13. M. Katono, T. Bessho, M. Wielopolski, M. Marszalek, J. E. Moser, R. H. Baker, S. M. Zakeeruddin, M. Gratzel, *J. Phys. Chem C*, **2012**, *116*, 16876–16884. <http://dx.doi.org/10.1021/jp304490a>
14. R. S. Verma, M. K. Swami, S. S. Manhas, P. K. Gupta, *Optics Commun.* **2010**, *283*, 2580–2587. <http://dx.doi.org/10.1016/j.optcom.2010.02.032>
15. D. Katsis, P. H. M. Chen, J. C. Mastrangelo, S. H. Chen, T. N. Blanton, *Chem. Mater.* **1999**, *11*, 1590–1596. <http://dx.doi.org/10.1021/cm9900397>
16. H. T. Srinivasa, S. Hariprasad, *Mol. Cryst. Liq. Cryst.* **2014**, *588*, 17–27. <http://dx.doi.org/10.1080/15421406.2013.822299>
17. R. Amaranatha Reddy, B. K. Sadashiva, *J. Mater. Chem.* **2004**, *14*, 310–319. <http://dx.doi.org/10.1039/b309262c>
18. H. T. Srinivasa, S. HariPrasad, *J. Organomet. Chem.* **2014**, *774*, 19–25. <http://dx.doi.org/10.1016/j.jorganchem.2014.09.037>
19. Bruker (2013). APEX2, SAINT and SADABS. Bruker AXS Inc., Madison, Wisconsin, USA.
20. G. M. Sheldrick, *Acta Cryst.* **2008**, *A64*, 112–122. <http://dx.doi.org/10.1107/S0108767307043930>
21. G. M. Sheldrick, *Acta Cryst.* **2015**, *C71*, 3–8.
22. L. J. Farrugia, *J. Appl. Cryst.* **2012**, *45*, 849–854. <http://dx.doi.org/10.1107/S0021889812029111>
23. C. F. Macrae, I. J. Bruno, J. A. Chisholm, P. R. Edgington, P. McCabe, E. Pidcock, L. Rodriguez-Monge, R. Taylor, J. Van de Streek, P. A. Wood, *J. Appl. Cryst.* **2008**, *41*, 466–470. <http://dx.doi.org/10.1107/S0021889807067908>

## Povzetek

Sintetizirali smo tekoče kristale (SmA) spojine 4-[4'-cianofenoksi-karbonil-fenil-4-(trimetilsilil)etnil]benzoata in jih karakterizirali z rentgensko strukturno analizo. Spojina kristalizira v triklnskem kristalnem sistemu, prostorski skupini P1; podatki osnovne celice:  $a = 5.9577(2)$  Å,  $b = 8.0398(3)$  Å,  $c = 25.8842(9)$  Å,  $\alpha = 86.096(2)^\circ$ ,  $\beta = 89.912(2)^\circ$ ,  $\gamma = 2.919(2)^\circ$ ,  $Z = 2$ , and  $V = 1182.16(7)$ . Kristalno strukturo stabilizirajo intra molekularne interakcije C–H...O. Prisotne so tudi šibke C–H... $\pi$  interakcije in tudi  $\pi$ – $\pi$  interakcije [centroid–centroid razdalja = 3.806 (3) Å].